Advances in Applied Energy 19 (2025) 100231

Contents lists available at ScienceDirect

Advances in Applied Energy

journal homepage: www.elsevier.com/locate/adapen

Net Zero without the gridlock through peer-to-peer coordinated flexibility

Wei Gan [a], Yue Zhou [a], Jianzhong Wu [a,*], Philip C. Taylor [b]

[a] School of Engineering, Cardiff University, Cardiff, CF24 3AA, United Kingdom
[b] Department of Electrical and Electronic Engineering, University of Bath, Bath, BA2 7AY, United Kingdom

ARTICLE INFO

Keywords:
Net zero
Low-voltage electrical distribution network
Distributed energy resources
Peer-to-peer coordinated flexibility
Statistically similar networks

ABSTRACT

In the pursuit of Net Zero, the rapid adoption of electric vehicles, heat pumps, and distributed generation is placing unprecedented pressure on low-voltage electrical distribution networks. Can these networks adapt and evolve without facing gridlock? Our study proposes an innovative peer-to-peer coordinated flexibility strategy that has the potential to significantly transform the landscape. By aggregating individual flexibility through peer-to-peer coordination, this approach enhances local power balance, mitigates gridlock, and safeguards individual benefits. Through a novel large-scale network analysis method based on statistically similar networks, we have quantified the maximal potential of peer-to-peer coordinated flexibility in alleviating gridlock and deferring network expansion. Using real-world UK low-voltage electrical distribution network data and authoritative distributed energy resources roadmaps, our findings reveal that peer-to-peer coordinated flexibility can reduce peak power flows by up to 20 % and enable as much as 91 % of UK residential low-voltage electrical distribution networks to meet peak demand without gridlock by 2050, significantly reducing the need for network expansion. Furthermore, with the adoption of peer-to-peer coordinated flexibility, the network's peak is projected to occur between 2045–2050, postponing it by 8–10 years compared to scenarios without it. These results underscore the critical role of peer-to-peer coordinated flexibility and serve as a benchmark for the co-development of future grids and flexible resources when addressing associated implementation challenges such as technological infrastructure and consumer engagement.

1. Introduction

Ever since the electrical revolution of the second half of the 19th century, centralised electricity generation has been predominant, encompassing various types of large-capacity power plants such as coal-fired and hydroelectric power plants [1,2]. However, the modern commitment to the Net Zero targets [3,4] has spurred a significant shift towards customer-side electrification, characterised by the rapid adoption of heat pumps [5] and electric vehicles (EVs) [6]. Simultaneously, distributed energy resources [7] (DERs, which include distributed generation [8,9], energy storage [10] and flexible demand [11]) are experiencing a considerable surge in popularity. When installed within low-voltage electrical distribution networks (LVDNs), DERs enable users to evolve from mere consumers of energy to 'prosumers', those who both consume and produce energy [12]. With a significant surge in electrical demand and DERs within LVDNs, electricity network elements, such as substations and electrical lines, are likely to experience capacity shortfalls, creating gridlocks that become bottlenecks and hinder the transition towards Net Zero [13]. This raises a critical question: can existing LVDNs accommodate the rapid and significant growth of demand and DER without gridlock? Although network expansion is the most straightforward solution to capacity shortfall [14], it brings about several significant issues. Firstly, large-scale network expansion could impose substantial costs on utility companies and governments, thus end users [15]. Secondly, nationwide expansion across all LVDNs may create supply chain and construction challenges. Furthermore, given the current severe gridlock in the transmission network, with 339GW of new generation in the UK queued for connections in a waiting list extending over a decade [16] to be connected, mere LVDNs expansion may not ensure sufficient and timely electricity supply to meet escalating demands.

Contrary to network expansion, one alternative strategy involves reducing capacity requirement by flexibility provision from local electrical demands and generation [17,18]. Flexible DERs such as battery storage and shiftable electrical demands [19] can provide flexibility, the capability of adjusting the demand or generation patterns of users for diverse benefits [20]. However, the effectiveness of these flexible DERs may be limited, primarily because they are small-scale and individually owned. When operated independently for individual benefit, without

* Corresponding author.
E-mail address: wuj5@cardiff.ac.uk (J. Wu).

https://doi.org/10.1016/j.adapen.2025.100231
Received 29 April 2025; Received in revised form 24 June 2025; Accepted 25 June 2025
Available online 29 June 2025

Nomenclature

Indices and Sets

Ω^{nonP2P}, Ω^{P2P} Set of nodes where households are outside or inside the P2P coalition

$S(i)$,$L_s(i)$,$L_e(i)$ Set of substations, lines starting or ending at node i

$s(l)$, $e(l)$ Starting and ending nodes of electrical line l

Parameters

ρ_t^{buy}, ρ_t^{sell} Buying and selling prices

r_l, x_l Line resistance and reactance

$\overline{E}_i^{batt}$, C_i^{batt} Energy capacity and asset value of battery storage at node i

$\overline{E}_i^{V2G}$, C_i^{V2G} Energy capacity and asset value of EV battery at node i

k Slope of the linear approximation of the percentage of capacity degradation as a function of the cycles

t_i^{in}, t_i^{out} Specific hour when EV at node i connects to or disconnects from grid

$\underline{V}_i$, $\overline{V}_i$ Allowable minimum and maximum values of nodal voltage

$\overline{S}_l$, $\overline{S}_s^{sub}$ Capacity limits for lines and substations

$P_{i,t}^{EV,dumb}$ Dumb charging load at node i and hour t

$P_{i,t}^{heat}$, $P_{i,t}^{other}$, $Q_{i,t}^{load}$ Heating, other loads, and reactive load at node i hour t

$\overline{P}_{i,t}^{PV}$, $E_{i,init}^{batt}$ Hourly available photovoltaic generation, initial energy of battery storage at node i

$E_{i,init}^{V2G}$, $E_{i,target}^{V2G}$ Initial or target energy of EV during grid connection

η^C, η^D Efficiencies during charging and discharging

$\overline{P}_i^{batt}$, $\overline{P}_i^{V2G}$ Maximum charge and discharge power of battery storage or EV battery

$\underline{P}_{i,t}^{heat}$, $\overline{P}_{i,t}^{heat}$ Upper and lower bounds allowed for the heating load at node i hour t

$\underline{P}_{i,t}^{other}$, $\overline{P}_{i,t}^{other}$ Upper and lower bounds allowed for the other load at node i hour t

D, IR Discount rate and the annual load growth rate obtained empirically

$Asset_s$, $Asset_l$ Asset value of substation s and line l

Variables

C^{buy}, R^{sell} Buying electricity cost or selling electricity revenue

$C^{\text{deg,batt}}$, $C^{\text{deg,V2G}}$ Degradation costs of battery storage and EV batteries

$P_t^{P2P,buy}$, $P_t^{P2P,sell}$ Power bought from or sold to the utility company of P2P coalition

$P_{i,t}^{takeG}$, $P_{i,t}^{feedG}$ Power taken from or fed to the network of household i

$P_{s,t}^{sub}$, $Q_{s,t}^{sub}$, $S_{s,t}^{sub}$ Active, reactive, and apparent power of substation s at hour t

$P_{l,t}$, $Q_{l,t}$, $S_{l,t}$ Active, reactive, and apparent power of line l at hour t

S_s^{sub}, S_l Maximum value of $S_{s,t}^{sub}$ or $S_{l,t}$ over the entire operating period

$P_{i,t}^{load}$, $P_{i,t}^{EV,smart}$, $V_{i,t}$ Active load, smart charging load and voltage at node i hour t

$P_{i,t}^{batt}$, $P_{i,t}^{PV}$, $P_{i,t}^{V2G}$ Outputs of battery storage, photovoltaic, and EV battery

$P_{i,t}^{D,batt}$, $P_{i,t}^{C,batt}$ Discharge or charge power of battery storage at node i hour t

$P_{i,t}^{D,V2G}$, $P_{i,t}^{C,V2G}$ Discharge or charge power of EV battery at node i hour t

$E_{i,t}^{batt}$, $E_{i,t}^{V2G}$ Stored energy in battery storage or EV battery at node i hour t

conscious coordination for grid needs, a situation known as individual flexibility, the potential of these flexible DERs in promoting local balance and mitigating gridlock remains limited [21–24]. Contrastingly, this paper introduces an innovative concept of peer-to-peer (P2P) coordinated flexibility, which allows multiple flexible DERs to collaborate, providing flexibility that serves grid benefits while safeguarding individual benefits, crucial for maintaining individual participation.

Instead of leaving DERs to operate independently, P2P coordinated flexibility harnesses the complementary nature of users' diverse DERs, significantly enhancing local power and energy balance. Implementing P2P coordinated flexibility not only safeguards individual benefits by minimising energy costs and maximising incomes for prosumers, but also provides network benefits, including mitigating network bottlenecks and deferring network expansion. To concretely implement coordinated flexibility, various methods can be utilised. P2P energy trading [25,26] is one such mechanism that enables energy network users to buy and sell electricity directly from each other within market-based frameworks [27,28]. When properly designed in a coordinated manner, it can avoid network congestion and node overloading that uncoordinated P2P transactions may cause, and instead benefit network operation in terms of network congestion, network flows, and other network-level benefits [25]. Despite the promising potential of P2P coordinated flexibility, it poses a critical question: can existing LVDNs, with the introduction of flexible DERs and P2P coordinated flexibility, accommodate the anticipated rapid growth of demands [29] and DERs [30] without experiencing gridlock or necessitating significant network expansion?

This paper not only firstly proposes the strategy of P2P coordinated flexibility, but also seeks to answer these questions by developing a novel method. This paper conducts a large-scale statistical and multiple-time-period analysis grounded in real-world UK electrical networks. This study harnesses actual network data from LVDNs in Stockport, a British city, coupled with credible future DER capacities from the Future Energy Scenarios (FES 2022) [30], a highly regarded publication issued by the UK National Grid. The main contributions are summarised as follows:

(1) This study digs into intricate details of network topologies, overcoming the limitations of oversimplified analyses ignoring network topologies. For such network analysis, depending solely on a single network or a limited number of representative networks is inadequate. Therefore, we devise a statistically similar network method to generate a large set of statistically similar networks based on actual British network data. These generated networks and real-world UK networks share statistically similar electrical and topological parameters, making them ideal for reliable statistical analysis.

(2) Furthermore, analyses are not only conducted for a single time period (e.g., 2050). Instead, they are carried out every five years from 2020 to 2050, providing a multiple-time-period evolution of LVDNs' capacity requirements with and without P2P coordinated flexibility.

(3) Our study finds that P2P coordinated flexibility is able to reduce peak flow of UK's LVDNs by approximately 20 % and enable 91 % of UK residential LVDNs to meet peak demand without gridlock by 2050, significantly reducing the need for network expansion.

(4) Additionally, network flows with P2P coordinated flexibility will peak around 2050, but that peak will be reached 8–10 years

earlier without it. These findings highlight the significant potential of P2P coordinated flexibility by quantifying its theoretical upper limits in reducing network capacity requirements.

Rather than addressing the full spectrum of implementation challenges associated with P2P coordinated flexibility, such as technological infrastructure or consumer engagement, this study focuses on using a robust approach, integrating our cutting-edge P2P coordinated flexibility-based LVDN analysis model and statistically similar network methods to quantify these theoretical upper limits. While practical performance may deviate from these theoretical estimates, understanding the maximum potential of P2P coordinated flexibility remains crucial. Overall, recognising that P2P coordinated flexibility is essential, this paper aims to quantify its maximum potential and provide valuable insights for evaluating its potential alongside conventional individual flexibility. These findings serve as a theoretical benchmark for researchers and policymakers in the co-development of future grids and flexible resources.

The overall structure of this paper is organised as follows. Section 2 introduces the concept of P2P coordinated flexibility. Section 3 examines the growing demand and DERs in UK residential distribution networks, along with their regional and scenario-based variations. Section 4 details the mathematical modelling and the statistically similar network method. Section 5 presents the main analysis results, focusing on how P2P coordinated flexibility reduces network flows and mitigates gridlock across substations and local lines. Sections 6–7 provide the discussion and conclusion.

2. Conceptual illustration of flexibility and P2P coordinated flexibility

Fig. 1 illustrates the concept of flexibility in electrical power systems and distinguishes between individual flexibility and P2P coordinated flexibility within LVDNs. Flexibility in electrical power systems refers to the ability to adapt to demand changes, supply fluctuations, network events (e.g. network component failures, voltage or frequency deviations), or other uncertainties to maintain balance between power supply and demand. Flexibility services can be provided by a range of sources including power plants, energy demand, energy storage and grid infrastructure. As shown in Fig. 1(a), flexibility services usually encompass two key technical aspects: firstly, the ability to rapidly adjust power exchange with the grid upwards or downwards in response to changes in generation, demand, network conditions or price signals; secondly, the ability to maintain these adjustments, either above or below a reference power level, over a specified duration, ensuring the provision of necessary power or energy adjustments, whether upwards or downwards.

In LVDNs, flexibility can be sourced from flexible DERs such as battery storage and shiftable electrical demands, which are owned by individual peers. Traditionally, each peer independently responds to signals from the flexibility buyer, providing what is known as individual flexibility, as illustrated in Fig. 1(b). In contrast, Fig. 1(c) demonstrates how P2P coordinated flexibility allows all peers to collectively provide flexibility through P2P coordination that promotes local power balance and significantly enhances network benefits. Detailed methodologies of P2P coordinated flexibility are described in the Method section.

This conceptual foundation underscores the necessity of coordinated flexibility, which becomes particularly critical given the rapidly increasing demand and DERs in UK residential distribution networks, as examined in the following section.

3. UK LVDN evolution and scenario analysis

3.1. Rising electrical demands and DERs in UK LVDNs

As stated by the UK National Grid FES 2022 [30], the UK LVDNs are

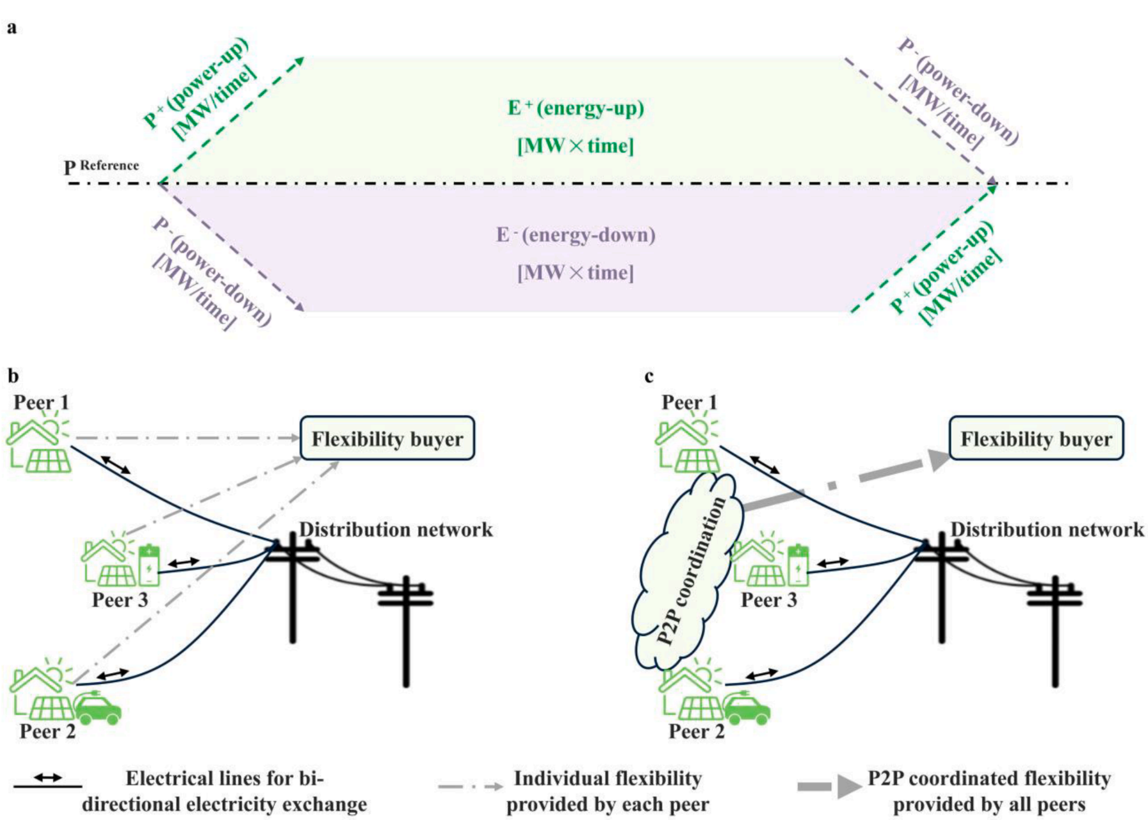

Fig. 1. Conceptual illustration of flexibility and comparison of different flexibility provision in LVDNs. **(a)** flexibility in electrical power systems; **(b)** individual flexibility in LVDNs; **(c)** P2P coordinated flexibility in LVDNs.

experiencing a rapid and dramatic increase in photovoltaic, battery storage, and electrical peak demands (e.g., due to heat pumps and electric vehicles). This paper focuses on residential LVDNs, excluding distribution networks that mainly supply commercial and industrial users. Fig. 2 portrays the anticipated evolution of the UK LVDNs from 2020 to 2050, highlighting a tenfold surge in residential photovoltaic capacity, from 4.1GW in 2020 to 40.7GW in 2050. With the rise of electric vehicles and heat pumps, peak residential electrical demands are projected to double from 18.6GW in 2020 to 38.4GW in 2050. Additionally, residential battery storage is projected to witness an astounding 280-fold increase, from 0.03GW to 8.4GW. Residential shiftable peak demand is also expected to surge from 0.04GW to 3.2GW, mitigating around 10 % of the 38.4GW peak demand in 2050. Apart from the residential shiftable peak demand like heat pumps, EVs can also provide flexibility through smart charging [31,32] and vehicle-to-grid [33] technologies, and the related data is provided in Fig. 2(e). For clarity, a supplementary information file containing data presented in the figures of this study is also available online [34].

While national trends highlight the scale of upcoming challenges, capturing system impacts requires consideration of regional heterogeneity and scenario-specific characteristics in DER deployment, which are explored in the next subsection.

3.2. Regional and scenario diversities in the UK

The previous section outlines the evolution of the UK LVDNs, spotlighting one of the four scenarios in FES 2022 [30], Leading the Way (LW). This scenario showcases the highest battery storage capacity and the lowest electrical demand, thanks to the improved efficiency of electrical demand. We also analyse the Customer Transformation (CT) scenario, which envisions the highest demand increase due to widespread electrification of heating and vehicles. In summary, the LW and the CT scenarios are selected as they respectively embody the highest increase in DERs and electrical demands. The other two scenarios, System Transformation and Falling Short, are not considered as they are deemed less relevant in the present development in the UK. Fig. 3(a) compares the peak demand and DERs of the LW and CT scenarios in 2050. The CT scenario displays a higher peak demand, while its battery storage capacity is lower than that of the LW scenario. Both scenarios suggest approximately 10 % of total peak demand to be shiftable.

Besides the distinct features of LW and CT, there exist notable regional variations in photovoltaic capacities and the initial loading levels (ILLs) of LVDN substations [30]. Fig. 3(b) illustrates regional per-household photovoltaic capacities in 2050, calculated by dividing the total residential photovoltaic capacities by household numbers [35]. Among them, "South West" leads with the highest per-household photovoltaic capacity of 3.6 kW, due to its considerable photovoltaic capacity and lower population density. The values in other regions range between 1.2 kW to 2.4 kW. This notable regional disparity is influenced by a combination of geographical advantages (e.g., higher solar irradiance), socio-economic factors such as household ownership rates and early adopter behaviours, as well as region-specific policy incentives that promote residential photovoltaic adoption. Fig. 3(b) also showcases the average ILLs of LVDN substations per region. These values, derived from thousands of realistic British substations, range between 54 % to 67 % [36–39]. Such data underscores the unprecedented challenges facing current LVDNs given the projected doubling of electrical demand and over a tenfold increase in photovoltaic capacity.

Figs. 2–3 outline the growth of demand and DERs and substations' ILLs of the UK LVDNs. By dividing the total DER capacity by the

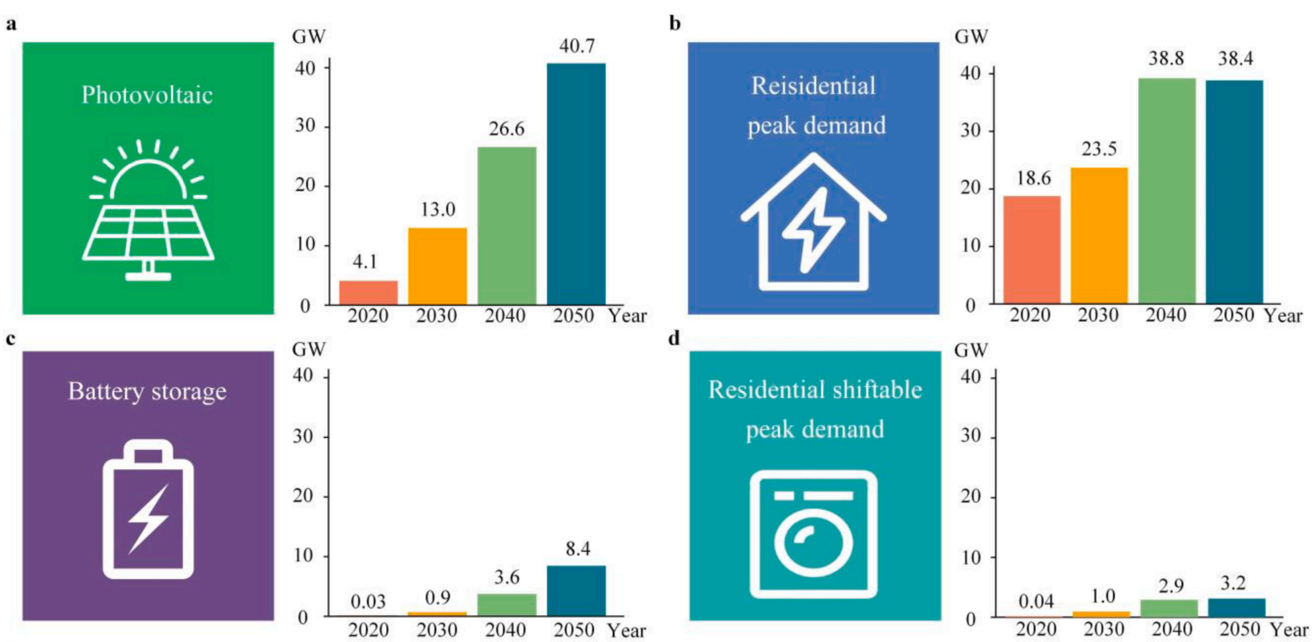

Year	2020	2030	2040	2050
Number of electric vehicles (million)	0.2	10.9	30.7	21.6
Percentages of electric vehicle owners participating in smart charge	31%	71%	91%	91%
Percentages of electric vehicle owners participating in vehicle-to-grid	0%	14%	29%	45%

Fig. 2. LVDN evolution over time in the UK [30]. **(a)** photovoltaic capacity growth; **(b)** peak demand growth; **(c)** battery storage growth; **(d)** peak demand that can be shifted into off-peak hours; **(e)** number of electric vehicles and percentages of electric vehicle owners participating in smart charging and vehicle-to-grid in different years in the UK. Smart charging encourages electric vehicle charging during off-peak hours, while vehicle-to-grid enables electric vehicles to feed electricity back into the grid.

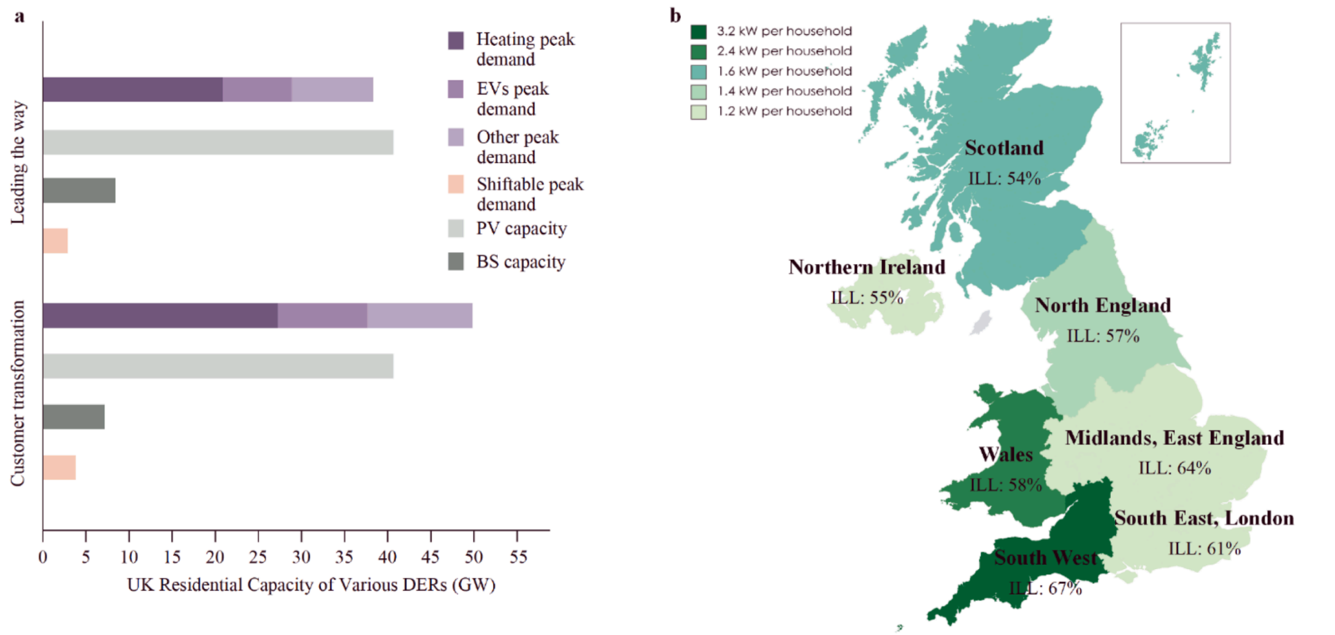

Fig. 3. Regional and scenario diversities in the UK. **(a)** capacities of residential DERs in 2050 under the LW and the CT scenarios; **(b)** average per-household photovoltaic capacity in 2050 and the initial loading levels (ILLs) of substations in various regions. Here, the ILL of a substation signifies the percentage of the available capacity that is occupied by the electrical demands and DERs in the initial year, specifically set as 2020 in this study.

household count, we estimate the average DER capacity per household and infer DER capacities for typical LVDNs based on their household numbers. Alongside these credible DERs parameters, this study utilises actual British LVDN network information, which is detailed in the following subsections.

This section characterises the rapid growth and regional diversity of future residential electricity demands and DERs in the UK. Building on these, the following Sections 4 and 5 present the method and assessment results on how P2P coordinated flexibility can mitigate rising network stress and defer the need for infrastructure expansion, respectively.

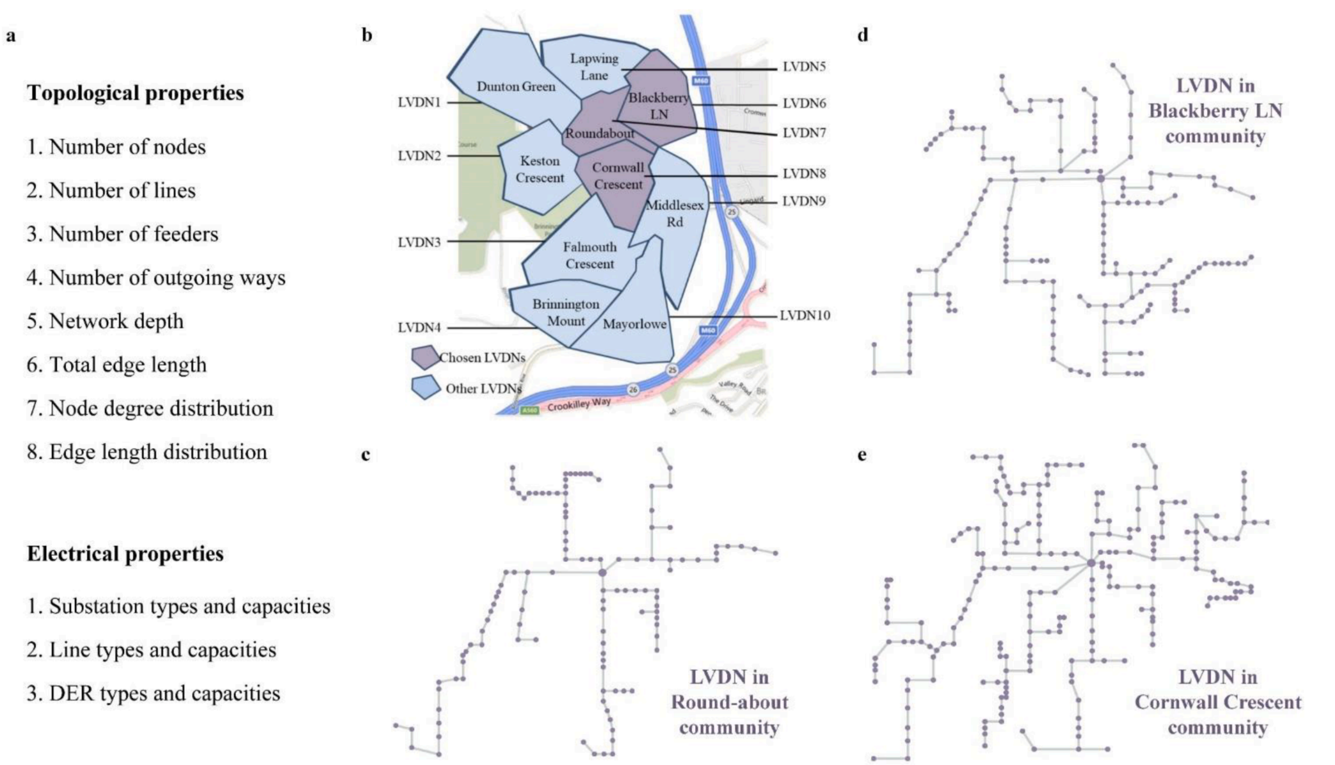

Fig. 4. Depictions of the statistically similar network method. **(a)** key topological and electrical properties of the UK residential LVDNs; **(b)** illustration of the actual British network in Stockport for validation; **(c)** topology of the LVDN, 'Roundabout'; **(d)** topology of the LVDN, 'Blackberry LN'; **(e)** topology of the LVDN, 'Cornwall Crescent'.

4. Method

4.1. Statistically similar network method

Statistically similar network method is a statistical tool, which is developed to generate any number of networks that maintain electrical and topological properties statistically similar to the realistic British residential LVDNs. The network properties include both topological (such as line depth, edge length properties) and electrical properties (such as line types and capacities), with key properties depicted in Fig. 4 (a). To ensure this method's capability in representing a wide range of network characteristics within the UK, residential LVDNs from Stockport are selected as inputs for the statistically similar network method. Specifically, from ten realistic residential LVDNs in Stockport, three are adopted with distinct topologies, reflecting the varied network characteristics and node counts (ranging from 120, 160, to 220) of different residential communities. The illustration of the adopted actual British network in Stockport is shown in Fig. 4(b), and three specific LVDNs, 'Roundabout', 'Blackberry LN', and 'Cornwall Crescent', are shown in Fig. 4(c)-Fig. 4(e).

The rationality for selecting typical networks from Stockport to represent UK residential LVDNs is threefold. Firstly, the UK Generic Distribution Networks developed by the Centre for Sustainable Electricity and Distributed Generation to represent UK medium or high-voltage distribution networks is also based on typical topological and electrical features and is widely regarded and used [41]. This provides evidence for using a similar method to represent LVDNs, which, like those medium or high-voltage networks, are also radial. Secondly, given the UK's urbanisation rate of 84 %, including both city centres and suburban areas, with suburbs comprising 55 % of the population [42], Stockport in the Greater Manchester area appropriately reflects the typical urban-suburban mix of the country. This makes its residential LVDNs suitable for representing the diverse LVDNs across the UK. Thirdly, both the electricity consumption and peak loads of these networks are consistent with the corresponding UK averages, and in terms of network characteristics, it has been analysed that networks in various UK regions exhibit similarities [43–45]. The rationality for selecting typical networks from Stockport further validates the effectiveness of the proposed statistically similar networks method in obtaining findings applicable to UK residential LVDNs. By applying our developed method for generating statistically similar networks, we can generalise selected actual British networks into any number of similar networks. Given the variability of scenarios across different years within the same network, more than tens of thousands of scenarios in this study are generated for analysis. Conducting analysis on these networks and scenarios ensures that our study's findings are not confined to a specific network or

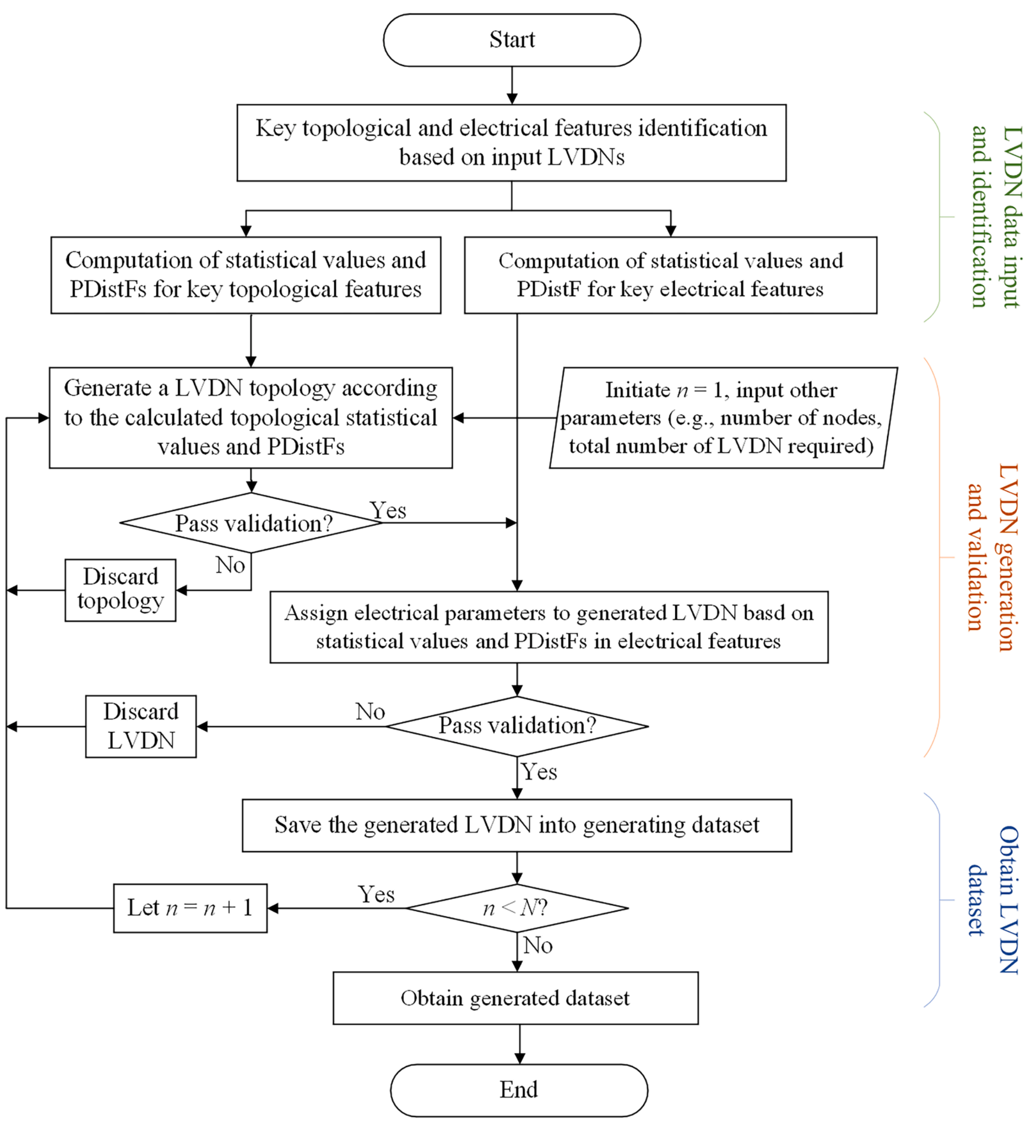

Fig. 5. Flowchart of the generation process of statistically similar LVDNs.

networks in a single region. Instead, they hold validity for the broad actual networks in the UK.

The method developed for generating statistically similar networks comprises two main stages: feature identification and network generation. The feature identification stage involves identifying key electrical and topological features from the input LVDNs and mathematically formulating their statistical features, primarily focusing on the probability distribution functions (PDistFs). The network generation stage aims to generate the network topology and assign electrical parameters to the generated topology, based on the previously identified and calculated statistical values and PDistFs for the key topological and electrical features. This whole process is systematically demonstrated in Fig. 5. The process begins with extracting statistical distributions for topological and electrical features from input networks. For each required LVDN, a topology is generated and validated against topological criteria. If successful, electrical parameters are then assigned and subjected to a second round of validation. Only networks that pass both validations are included in the final dataset, ensuring statistical similarity to actual LVDNs. The detailed mathematical formulation of the feature identification and network generation process, as well as the validation methods, is provided in Appendix A.

Stochastic generation of DER geographical distributions and capacities. Numerous scenarios with varying DER geographical distributions and capacities throughout the entire UK network are generated based on the data shown in Fig. 2. Specifically, the spatial distributions of DER installations are formulated through simple random sampling from a subset of nodes identified as potential DER locations, which reflects spatial clustering and avoids uniform deployment across all nodes. For these selected nodes, the individual DER capacities, which include battery storage, photovoltaic, and EVs, are developed under the presumption of adherence to uniform distributions. The upper and lower bounds of these uniform distributions, representing DER capacities per household, are extrapolated from the data depicted in Fig. 2[30].

4.2. P2P coordinated flexibility-based LVDN analysis model

The two-stage analysis model. A two-stage analysis model is developed under the assumption that all P2P participants are coordinated to reduce the overall electricity cost and power flows, with the first stage minimising the electricity cost of the LVDN users and the second optimising the proposed flow indicator.

Objective of the first-stage model. The first-stage problem aims to minimise the total cost for all households in the LVDN, taking into account the degradation cost of battery storage. As demonstrated in Eq. (1), the objective comprises four components: the cost of buying electricity from the utility company and the revenue of selling electricity back to the utility company, as well as degradation costs of batteries in battery storage systems and EVs offering vehicle-to-grid services. The model assumes that P2P participants can share electricity with one another as well as forming a coalition to trade electricity with the utility company, whereas non-P2P households trade electricity with the utility company independently. Eqs. (2) and (3) represent the total electricity purchasing cost and selling revenue. In the Full P2P case, the set $\Omega^{\mathrm{non}P2P}$ is empty. However, in the No P2P case, all households within the adopted LVDN are included in the set. The degradation cost of battery storage is represented by Eq. (4). Here, it is assumed that the battery life and capacity are proportional to the charge and discharge cycles of batteries [47]. Typically, within the whole operational period, the total electricity discharged from the battery storage is roughly equivalent to the total electricity charged when disregarding the efficiency loss, and the number of charge and discharge cycles during the operational period can be estimated by dividing the cumulative discharged electricity by the battery's energy capacity. Similarly, Eq. (5) measures degradation costs for EV batteries offering vehicle-to-grid services.

$$\min\ C^{total} = C^{buy} - R^{sell} + C^{\mathrm{deg,batt}} + C^{\mathrm{deg,V2G}} \tag{1}$$

$$C^{buy} = \sum_{t=1}^{T} \rho_t^{buy} \left(P_t^{P2P,buy} + \sum_{i \in \Omega^{nonP2P}} P_{i,t}^{takeG} \right) \tag{2}$$

$$R^{sell} = \sum_{t=1}^{T} \rho_t^{sell} \left(P_t^{P2P,sell} + \sum_{i \in \Omega^{nonP2P}} P_{i,t}^{feedG} \right) \tag{3}$$

$$C^{\mathrm{deg,batt}} = \sum_i \frac{k}{100} C_i^{batt} \left(\sum_{t=1}^{T} P_{i,t}^{D,batt} \Big/ \overline{E}_i^{batt} \right) \tag{4}$$

$$C^{\mathrm{deg,V2G}} = \sum_i \frac{k}{100} C_i^{V2G} \left(\sum_{t \in \left[1, t_i^{out}\right] \cup \left(t_i^{in}, T\right]} P_{i,t}^{D,V2G} \Big/ \overline{E}_i^{V2G} \right) \tag{5}$$

The first-stage model is subject to energy trading constraints, power flow constraints, battery storage operational constraints, and flexible load operational constraints. The detailed mathematical formulations of these constraints are provided in Appendix B.

Objective of the second-stage model. Before delving into the second-stage model, it's notable that the first-stage model gets the minimised total cost (C^{total}) of all households with the determination of power load ($P_{i,t}^{load}$) and electricity outputs from electric vehicles providing vehicle-to-grid services ($P_{i,t}^{V2G}$), photovoltaic systems ($P_{i,t}^{PV}$), and battery storage ($P_{i,t}^{batt}$) for households located at each node for each hour. Since the values of these variables are obtained through the optimisation in the first-stage model, we will rename these obtained values as $C^{total,1st}$, $P_{i,t}^{load,1st}$, $P_{i,t}^{V2G,1st}$, $P_{i,t}^{PV,1st}$, $P_{i,t}^{batt,1st}$, respectively. Although the first-stage model achieves the optimal total cost, it does not involve any optimisation of the power flow within the LVDN. However, as long as the total cost is not increased, the P2P participants are willing to flexibly adjust their power load and electricity outputs from different DERs, while surplus electricity can be shared with other P2P participants. In this manner, the DERs of P2P participants can be re-optimised to bring about network benefits and optimise power flow, without any additional cost increment. Therefore, the second-stage model is formulated for the re-optimisation of DERs of P2P participants, with the objective of minimising the overall power flow across the LVDN. Here, a power flow quantification indicator is proposed to measure the importance of a device, employing the asset value of the device (including substations and electrical lines) and the degree of urgency which is determined by the ratio of maximum loading to device capacity. The power flow quantification indicator for substation s is denoted as L_s and for line l is denoted as L_l. The overall objective function is the sum of all the power flow quantification indicators as shown in Constraint (6). The definitions of L_s and L_l are given in Eqs. (7) and (8).

$$\min \sum_s L_s \left(S_s^{sub} \big/ \overline{S}_s^{sub} \right) + \sum_l \mathrm{L}_l \left(S_l \big/ \overline{S}_l \right) \tag{6}$$

$$S_s^{sub} = \max_t S_{s,t}^{sub}, \quad \mathrm{L}_s \left(S_s^{sub} \big/ \overline{S}_s^{sub} \right) = \frac{Asset_s}{(1+D)^{\log\left(S_s^{sub} / \overline{S}_s^{sub}\right) / \log(1+IR)}} \tag{7}$$

$$S_l = \max_t S_{l,t}, \quad \mathrm{L}_l \left(S_l \big/ \overline{S}_l \right) = \frac{Asset_l}{(1+D)^{\log(S_l / \overline{S}_l) / \log(1+IR)}} \tag{8}$$

The second-stage operational constraints. All operational constraints present in the first-stage model (i.e., Constraints (2–5) and Constraints (B.1-B.19)) are also considered in the second-stage model. In addition, several constraints outlined in Eqs. (9)-(10) are introduced in the second-stage model. Specifically, Eq. (9) ensures that the total cost calculated in the second stage is consistent with that in the first stage. Eq. (10) indicates that for households not participating in P2P energy trading, the determinations of their power loads and power outputs of various DERs should remain consistent with those in the first stage.

$$C^{total} = C^{total,1st} \tag{9}$$

$$P_{i,t}^{load} = P_{i,t}^{load,1st}, \quad P_{i,t}^{V2G} = P_{i,t}^{V2G,1st}, \\ P_{i,t}^{PV} = P_{i,t}^{PV,1st}, \quad P_{i,t}^{batt} = P_{i,t}^{batt,1st}, \quad \forall t, \forall i \in \Omega^{nonP2P} \tag{10}$$

To clarify the modelling and control assumptions for the three cases introduced earlier (Full P2P, No P2P, and No Flex), the following configurations are applied. In the Full P2P case, all households are assigned to the P2P coalition. In the No P2P case, all households belong to the non-P2P coalition. Aside from this difference in coalition structure, the modelling formulations remain otherwise identical. In the No Flex case, all households are assigned to the non-P2P coalition, and all flexible DER capacities are set to zero. Specifically, battery storage is disabled, EVs operate under dumb charging only, and shiftable loads, including heating and other flexible demands, are fixed to baseline hourly demand, effectively eliminating temporal shifting.

5. Case study

5.1. *Deferring peak network flows through P2P-coordinated flexibility*

This study develops a P2P coordinated flexibility-based large-scale LVDN analysis method (see Method section for details) to analyse the role of P2P coordinated flexibility in mitigating gridlock and deferring network expansion. The following three cases are analysed and compared, with modelling assumptions and distinctions outlined in the Method section.

No Flex: Neither battery storage nor flexibility from electrical demands are considered.

No P2P (Individual Flexibility): Flexible DERs are considered but without P2P coordination. Only individual user benefits are considered during the analysis, excluding grid benefits.

Full P2P (P2P Coordinated Flexibility): Flexible DERs are incorporated with P2P coordination to consider both individual user benefits and grid benefits.

Fig. 6 illustrates the maximum substation power flow reduction in the UK residential LVDNs under both the LW and the CT scenarios via P2P. Lowering maximum substation power flow effectively reduces required network capacities. In the No Flex case, the maximum substation power flow, depicted as the highest value observed throughout the year, increases significantly due to the surging electrical demands. In the No P2P case, uncoordinated flexible DERs mitigate the corresponding maximum substation power flow by 11 % under the LW scenario, as shown in Fig. 6(c). Meanwhile, under the LW scenario, P2P further reduces the maximum peak substation power flow by an additional 21 % compared to that of the No P2P case, while under the CT scenario, P2P brings an additional 17 % reduction. Notably, in the Full P2P case, the annual maximum substation power flow peaks in 2045 under the LW scenario and in 2050 under the CT scenario. By contrast, the No P2P cases reach the same values 8.1 years earlier under the LW scenario and 10.2 years earlier under the CT scenario. In summary, the network power flow peaks in 2045–2050 with P2P but reaches the same values 8–10 years earlier without P2P.

Notably, our findings for each year and each case are presented as a range of values based on the analysis results of a large number of statistically similar networks, not as a single data point, as visualised in Fig. 6(a-b). The bar chart represents the average value, while the short horizontal lines above and below each bar denote the maximum and the minimum values of the range. These three statistical values (maximum, minimum, and average) are derived from large-scale network analysis results. Specifically, this is made possible through the developed statistically similar network generation method, which generates a set of simulated networks that share statistically similar electrical and topological features with the actual British networks, thus guaranteeing the practical applicability of the analysis results. Conducting analyses on these networks ensures that the findings are broadly applicable, rather than being confined to a specific network.

The analysis above demonstrates how P2P coordinated flexibility can defer peak network flows and delay capacity bottlenecks. Building on this, the next subsection investigates the extent to which this strategy

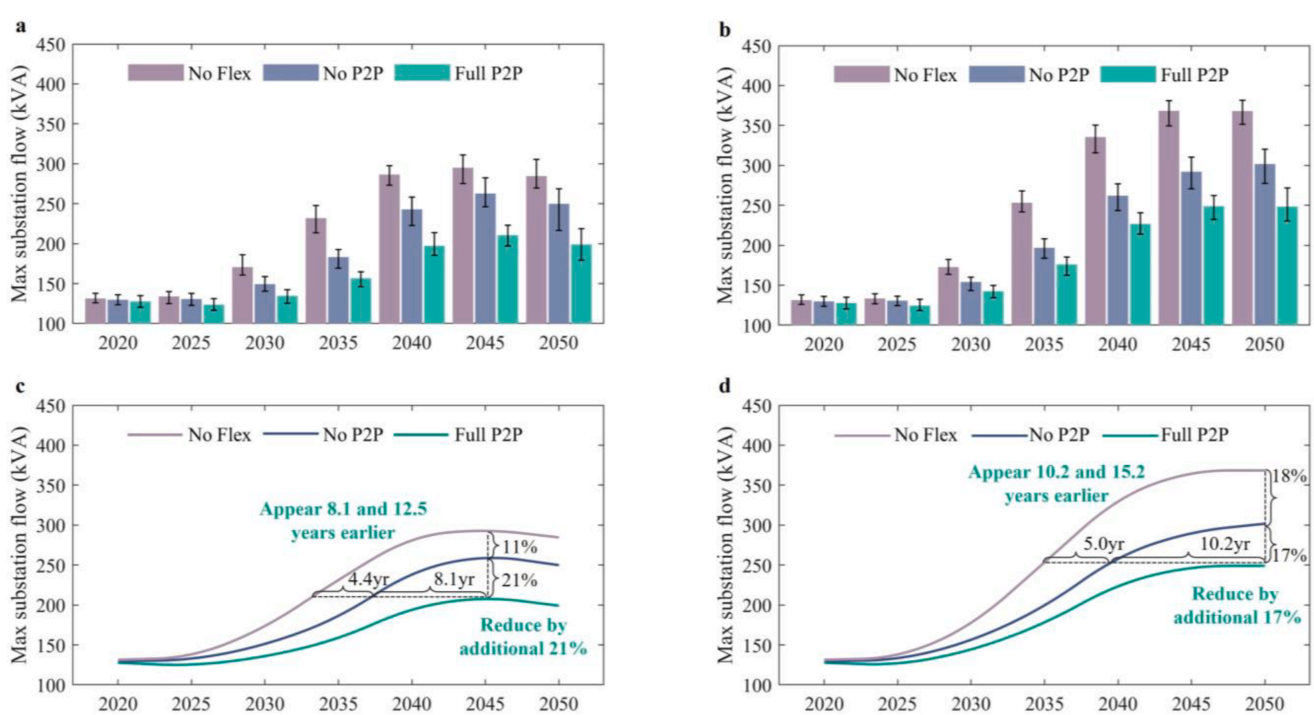

Fig. 6. Potential of P2P in max substation power flow reduction and deferral years of peak network power flow. **(a)** comparison of the maximum substation power flow of different cases in different years under the LW scenario; **(b)** comparison of the maximum substation power flow of different cases in different years under the CT scenario; **(c)** analysis of the maximum substation power flow reduction and peak network power flow deferral years under the LW scenario; **(d)** analysis of the maximum substation power flow reduction and peak network power flow deferral years under the CT scenario.

could allow residential distribution networks across the UK to accommodate rising peak demand without requiring expansion.

5.2. P2P coordinated flexibility enables meeting growing peak demand without gridlock

Following the above analysis, this section aims to answer what percentage of the UK residential LVDNs could avoid network expansion by 2050. Fig. 7, under the LW scenario, showcases forecasted future loading levels (FLLs) of the residential LVDNs in various UK regions for both No P2P and Full P2P cases in 2050. Illustrated in Fig. 7(a), in the No P2P case, all regional residential LVDNs' FLLs are projected to exceed the 100 % network capacity by 2050, indicating that network expansion will be inevitable across the whole UK. These findings align with Figs. 2–3, which suggest that the current UK residential LVDNs, with ILLs over 50 %, will face challenges in accommodating a doubling of electrical demand and a tenfold increase in photovoltaic capacities.

Fig. 7(b) shows the residential LVDNs' FLLs of various UK regions, and the Full P2P case is significantly different from the No P2P case. In the Full P2P case, residential network expansion is avoided in six out of seven regions. The "South West" region is the sole exception that necessitates network expansion, as its per-household photovoltaic capacity is nearly triple that of the other regions. The other six regions experience a significant reduction in FLLs in the Full P2P case, with values remaining under 100 %. This signifies that a considerable portion of the UK residential LVDNs is able to avoid network expansion through P2P. Given that these six regions represent 91 % of the UK's population, it is reasonable to roughly estimate that P2P could enable approximately 91 % of the UK residential LVDNs to meet peak demand without gridlock by 2050. While this does not entirely eliminate the need for network expansion upgrades given the additional practical need for resilience and robustness against uncertainties, these LVDNs without gridlock would still require significantly less investment compared to the grid-congested LVDNs that would emerge without P2P coordination.

While the previous subsection demonstrates how P2P coordinated flexibility can enable a large share of residential networks to meet peak demand without gridlock, the following subsection further examines its benefits by analysing how it reduces power flows not only at substations but also along local electrical lines across the network.

5.3. Power flow reduction for both substations and local electrical lines

Figs. 6–7 highlight the potential of P2P in mitigating gridlock at the substation level. Fig. 8 further extends the analysis by focusing on local electrical lines within the residential LVDNs and provides a detailed spatial-temporal analysis of the power flow reduction. Fig. 8(a) introduces a topological concept, line depth, which is defined in the legend of Fig. 8. Fig. 8(b) showcases numerous curves for both No P2P and Full P2P cases. Each curve represents the result for one of the generated networks that is statistically similar to the actual British networks. The average curves, depicted as bold lines, illustrate a significant reduction in maximum line power flow with P2P, irrespective of the line depth. The gap between the curves represents an average relative reduction of around 20 %, a ratio consistently maintained across the line depths (Fig. 8(c)). This suggests P2P's effectiveness in reducing the maximum line power flow and mitigating gridlock within the residential LVDN, regardless of the line depth or location. Additionally, the trends suggest potential benefits even for higher voltage level electrical lines outside the LVDNs, further highlighting the potential of P2P in deferring network expansion.

Fig. 8(d) provides a more detailed spatial-temporal analysis, showing how power flow reduction varies with both the line depth and percentile rank. In contrast to Fig. 8(b), which only focuses on the maximum power flow among 8760 hours' values throughout the year, Fig. 8(d) provides key percentile points from the 10th to the 100th percentile among these 8760 values. For instance, the 80th percentile point is the value that is greater than exactly 80 % of the yearly 8760 values. The figure reveals that the greatest reduction occurs at the 100th percentile point, with less

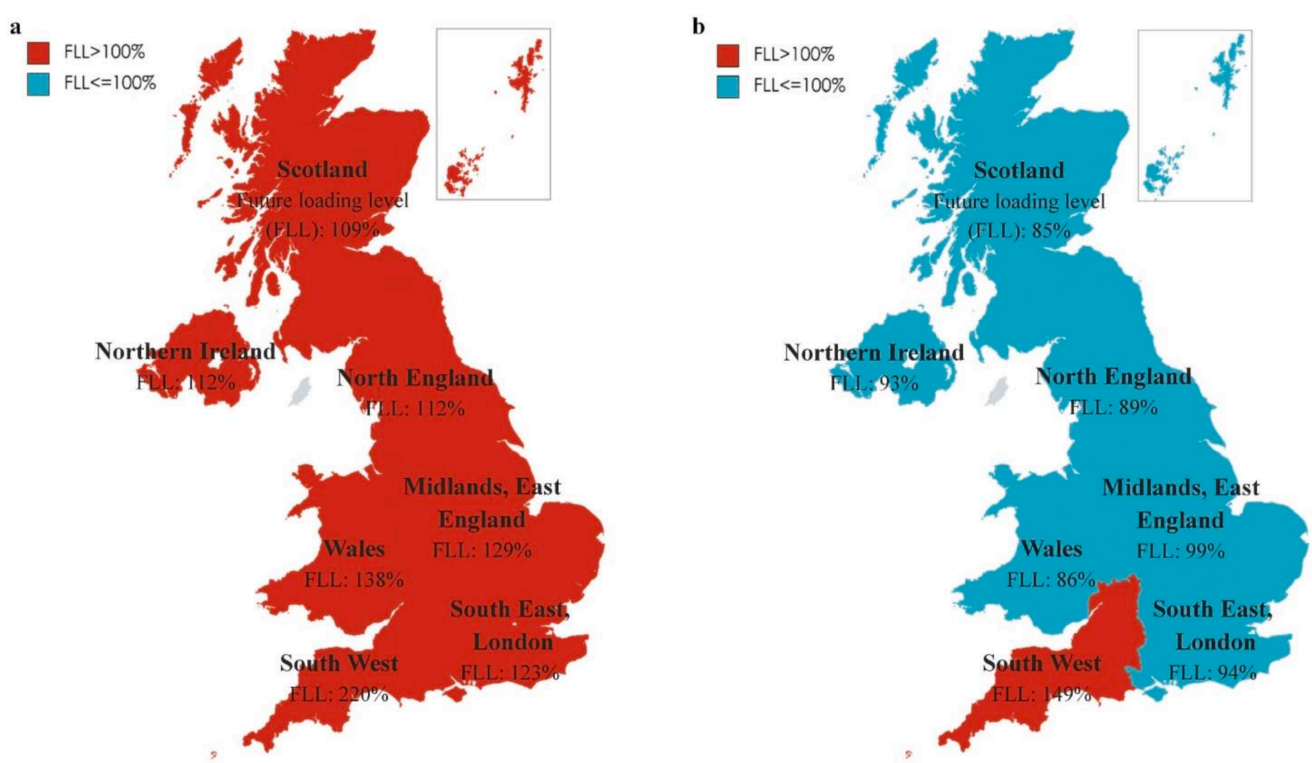

Fig. 7. FLLs and indication of whether network expansion is required in different regions in the UK in 2050 under the LW scenario. Here, the FLL of a substation, in contrast to the ILL which captures the substation's initial status in 2020, signifies the percentage of its available capacity that is occupied by the electrical demands or DERs in a future year, specifically chosen as 2050 in this study. **(a)** No P2P case; **(b)** Full P2P case.

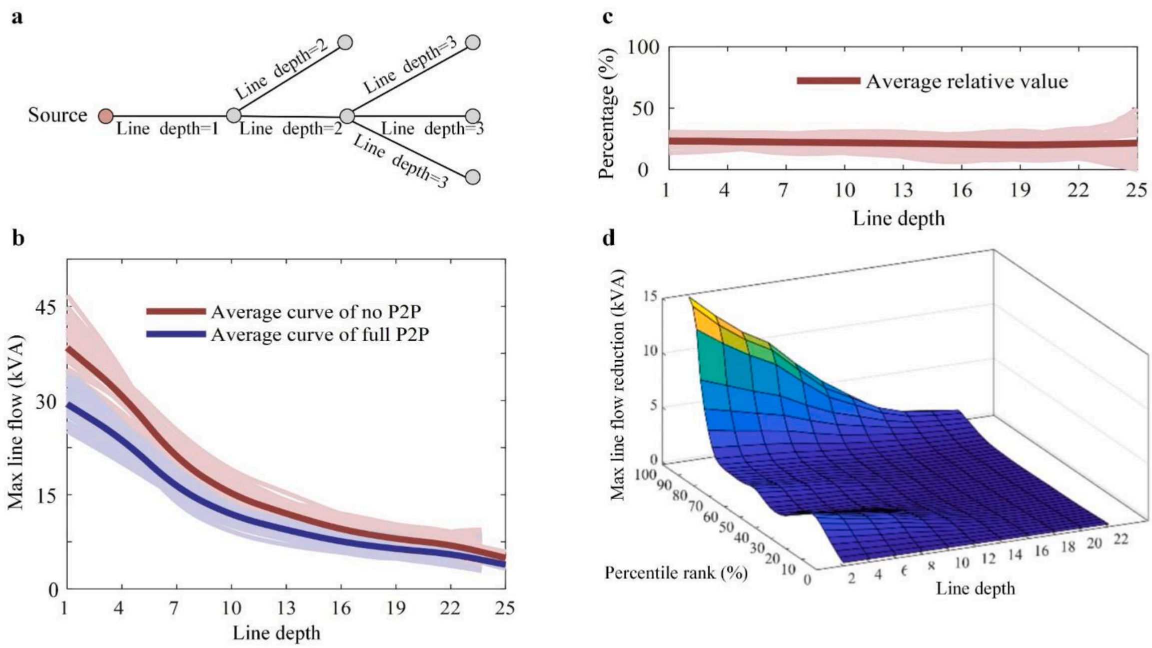

Fig. 8. Spatio-temporal analysis of the max line power flow comparison between the No P2P and Full P2P cases under the LW scenario in 2050. Here, the line depth is determined by the shortest path's line count from the network's substation to this node. **(a)** a simple network for illustration of the line depth; **(b)** percentage power flow differences between No P2P and Full P2P cases for various line depths; **(c)** the maximum power flow comparison between No P2P and Full P2P cases for various line depths; **(d)** the maximum power flow differences between No P2P and Full P2P cases as a function of line depth and percentile rank.

significant reductions at other points. This indicates that P2P reduces network capacity requirements by effectively reducing line power flow during peak hours. In summary, Figs. 6–8 collectively demonstrate that P2P benefits both substations and local electrical lines in alleviating gridlock and delaying network expansion.

6. Discussion

Rather than addressing the full spectrum of implementation challenges, such as technological infrastructure or consumer engagement, these findings highlight the significant potential of P2P coordinated flexibility by quantifying its theoretical upper limits in reducing network capacity requirements. Regarding the realistic implementation of P2P coordinated flexibility, substantial progress has been made in overcoming the technical hurdles, supported by recent research on control, market mechanisms and distributed settlement technologies. The main area that requires further development pertains to policy regulation and new business models. Yet, as the practical value of P2P projects continues to be affirmed through real-world applications, it is expected that policy acceptance will grow and effective business models to implement P2P will be further developed. In summary, our proposed P2P coordinated flexibility represents an efficient, cost-effective, easy-to-implement solution, serving as a highly appealing alternative or supplement to network expansion and aiding in paving the path to Net Zero, with our quantitative findings providing valuable insights and serving as a benchmark for researchers and policymakers in the co-development of future grids and flexible resources. For real implementation, further research is needed to understand how to ensure the enthusiasm of users to participate in P2P coordination, and how to quantify and demonstrate the unique advantages of P2P coordination in terms of users' participation motivation and fairness.

7. Conclusion

This study delves deeply into the developments and challenges faced by the UK's residential LVDNs as the country progresses towards Net Zero. Given that the current capacity utilisation of the UK's residential LVDNs already exceeds 50 %, accommodating more than double the existing electrical demand and an over tenfold increase in photovoltaic generation presents a significant challenge. Moreover, in light of the severe gridlock in the transmission and distribution networks, achieving local power and energy balance and mitigating gridlock for LVDNs becomes even more crucial. Our study introduces a novel method, implementing P2P coordinated flexibility to coordinate flexible DERs, that significantly contributes to gridlock mitigation. Importantly, we have quantified the potential of P2P coordinated flexibility in mitigating gridlock and delaying network expansion through a novel large-scale statistically similar network analysis method considering P2P coordinated flexibility.

This study employs actual British residential electrical distribution networks and authoritative DER roadmaps, ensuring our results authentically reflect the realistic conditions and possible evolution of the residential LVDNs. These analyses are based on networks that are generated using our statistically similar network method, where data are drawn from actual British networks. These simulated networks share statistically similar electrical and topological features with that of the actual British networks, thus guaranteeing the practical applicability. Additionally, generalising several actual British networks into large-scale statistically similar networks further extends their representativeness. Conducting analysis on these networks ensures that the findings are not confined to a specific network. Instead, they hold broad validity for any actual networks, either in the UK or globally, that demonstrate distinct statistical similarity to the generalised networks in both topological features and electrical parameters. The study finds that P2P coordinated flexibility could reduce the peak power flow by around 20 % and enable up to 91 % of the UK residential LVDNs to meet peak demand without gridlock by 2050. This study also reveals the role of P2P coordinated flexibility in deferring the increase of network power flow, which peaks in 2045–2050 with P2P coordinated flexibility but reaches the same values 8–10 years earlier without it. Furthermore, the analysis demonstrates the effectiveness of P2P coordinated flexibility in mitigating gridlock, not only within the context of substations but also local electrical lines within the residential LVDNs.

Delving deeper into the findings, the substantial benefits of P2P coordinated flexibility become more evident. 1) P2P coordinated flexibility could potentially enable up to 91 % of the UK residential LVDNs to meet peak demand without gridlock. While this does not entirely eliminate the need for network expansion upgrades, these gridlock-free LVDNs would still require significantly less investment, leading to substantial cost savings compared to the grid-congested LVDNs that would emerge without P2P coordination. For example, Northern Powergrid, a distribution network operator serving 8 million people in the UK, plans a £405 million network expansion from 2023 to 2028 [40]. Assuming P2P coordination is theoretically able to reduce such investment needs by up to 91 %, it could result in potential savings of approximately £369 million. Applying this across the UK's entire electricity distribution network serving 67 million people, total savings could reach £3.1 billion over a mere five years. 2) While substantial cost savings are a key benefit of P2P coordinated flexibility, its advantages go far beyond just financial gains. It also addresses the considerable challenges tied to large-scale LVDN expansions, such as those involving procurement, manufacturing, and construction work. In comparison to network expansion, P2P coordinated flexibility deployment is simpler and more cost-effective due to the affordable and easy-to-install metering, control and communication devices. 3) Given the severe gridlock in the transmission network, with 339GW of new generation waiting for connections in a long queue, even successful LVDN expansion may fall short to meet escalating demands due to the transmission network's limited capacity. P2P coordinated flexibility can alleviate this issue through promoting local electricity power and energy balancing, thus reducing the LVDNs' reliance on the congested transmission network. 4) The uncertainties of future demand and DERs growth introduces further complexity. Premature or excessive investment in network expansion could lead to inefficient resource allocation. Conversely, P2P coordinated flexibility provides a flexible response to these uncertainties. Its ability to defer network power flow growth and enable rapid deployment allows more informed decision-making on future electrical distribution network investments.

Code availability

The code from this study will be available upon request.

CRediT authorship contribution statement

Wei Gan: Writing – original draft, Visualization, Validation, Methodology, Data curation. **Yue Zhou:** Writing – review & editing, Methodology, Investigation. **Jianzhong Wu:** Writing – review & editing, Supervision, Project administration, Funding acquisition, Conceptualization. **Philip C. Taylor:** Writing – review & editing, Funding acquisition.

Declaration of competing interest

The authors claim no conflicts of interest.

Acknowledgements

This research was funded by the UK's Engineering and Physical Sciences Research Council under Grant EP/Y016114/2 (Supergen Energy Networks Impact Hub).

Supplementary materials

Supplementary material associated with this article can be found, in the online version, at doi:10.1016/j.adapen.2025.100231.

Appendix A: Supplementary mathematical formulation for the statistically similar network method

The feature identification stage, taking input from LVDNs, focuses on calculating the PDistFs for key topological and electrical features such as node degree (the number of edges directly connected to node i), edge length, and nodal peak load. Specifically, Equation (A.1-A.3) details the node degree's probability mass function. Here, $\boldsymbol{A}$ represent the adjacency matrix, where element A_{ij} signifies if nodes i and j are connected (1 for connected, 0 for not). With N representing the total node count, $\boldsymbol{A}$ forms an $N \times N$ matrix. The degree of node i, d_i, is given in Equation (A.1). Using k as the index for potential node degrees, the number and probability of nodes with a degree of k are represented as $n(k)$ and $pr(k)$, detailed in Equation (A.2) and (A.3), respectively. In contrast to node degree, the edge length's distribution is captured as a probability density function and characterised by an exponential distribution in Equation (A.4). Here, μ is the coefficient of the exponential distribution, m denotes edge length, while $m_{\min}$ and $m_{\max}$ specify the minimum and maximum edge length values from the input network data. For nodal peak load, due to its varied values, a kernel density probability distribution is derived as shown in Equation (A.5). This kernel density estimation, a non-parametric method, aids in describing distributions that can't be easily characterised by common distributional forms. Here, a Gaussian kernel density function $K(x)$ is employed, where x represents the nodal peak load. The bandwidth, h, is pivotal in determining the smoothness of the estimate, and x_i are the data points sourced from the input networks.

$$d_i = \sum_{j=1}^{N} A_{ij},\ i \in [1, 2, \ldots, N] \tag{A.1}$$

$$n(k) = \sum_{i=1}^{N} 1_{\{d_i = k\}},\ k \in [1, 2, \ldots, \max\{d_1, d_2, \ldots, d_N\}] \tag{A.2}$$

$$pr(k) = \frac{n(k)}{N},\ k \in [1, 2, \ldots, \max\{d_1, d_2, \ldots, d_N\}] \tag{A.3}$$

$$pr(m) = \begin{cases} \frac{1}{\mu} e^{-\frac{1}{\mu}} & m \in [m_{\min}, m_{\max}] \\ 0 & m \notin [m_{\min}, m_{\max}] \end{cases} \tag{A.4}$$

$$pr(x) = \frac{1}{N \cdot h} \sum_{i=1}^{N} K\left(\frac{x - x_i}{h}\right), \quad K(x) = \frac{1}{\sqrt{2\pi}} e^{-\frac{x^2}{2}} \tag{A.5}$$

Using these probability distribution functions, which capture both the key topological and electrical features of LVDNs, the generation of statistically similar LVDNs is formulated in a systematic and structured manner. The network generation stage initiates with the generation of a network topology, informed by the PDistFs of topological features and specific parameters such as the desired number of generated LVDNs and the total node count in the LVDN. Subsequently, this topology undergoes a validation to ensure its topological features align with those identified from the input LVDNs. Topology not passing validation is discarded and a new one is generated. Once a topology passes this validation, it is then supplemented with electrical parameters like substation capacities and nodal peak loads. Moreover, line parameters, including line capacities and impedance, are designated appropriately. A validation is also conducted to ensure that the generated network, with its assigned electrical parameters, exhibits topological and electrical features that are statistically similar to those of the input LVDNs. Once the network passes this validation, it is then included into the network generating dataset. Through the developed network generation method, the findings obtained from the generated statistically similar LVDNs can be deemed reliable and applicable for a wide range of real-world LVDNs.

To quantitatively verify the representativeness of these statistically similar networks, we employed multiple graph-theoretic similarity metrics, including cosine similarity, spectral similarity, and graph edit distance, as introduced in our previous study [46]. These metrics are used to filter and validate the generated networks, ensuring that they are statistically aligned with the key electrical and topological characteristics observed in actual UK residential LVDNs.

Appendix B: Supplementary mathematical formulation for LVDN analysis model

Energy trading constraints of the first-stage model. The power taken from or power fed to the network for each household is represented by Equation (B.1). Equation (B.1) also ensures that, for any specific node and hour, either $P_{i,t}^{takeG}$ or $P_{i,t}^{feedG}$ must be zero. Equation (B.2) is used to calculate the hourly purchased (sold) energy of the entire P2P coalition from (to) the utility company for P2P participants. Furthermore, it ensures that, for any specific hour, either $P_t^{P2P,buy}$ or $P_t^{P2P,sell}$ must be zero. It is notable that all these households are all located within the same substation, with some even sharing the same feeder, thereby offering substantial potential to reduce power flow in the substation and associated electrical lines. Constraint (B.3) ensures these variables are non-negative.

$$\begin{aligned} P_{i,t}^{takeG} - P_{i,t}^{feedG} &= P_{i,t}^{load} - P_{i,t}^{V2G} - P_{i,t}^{PV} - P_{i,t}^{batt}, \\ P_{i,t}^{takeG} \cdot P_{i,t}^{feedG} &= 0 \quad \forall t, \forall i \end{aligned} \tag{B.1}$$

$$\begin{aligned} P_t^{P2P,buy} - P_t^{P2P,sell} &= \sum_{i \in \Omega^{P2P}} \left(P_{i,t}^{takeG} - P_{i,t}^{feedG}\right), \\ P_t^{P2P,buy} \cdot P_t^{P2P,sell} &= 0 \quad \forall t \end{aligned} \tag{B.2}$$

$$P_{i,t}^{takeG},\ P_{i,t}^{feedG},\ P_t^{P2P,buy},\ P_t^{P2P,sell} \geq 0 \quad \forall t, \forall i \tag{B.3}$$

Power flow constraints of the first-stage model. An Alternating Current (AC) power flow model is utilised to calculate the power flow. The constraints for active and reactive power balances are expressed as Equations (B.4) and (B.5). Because usually there is only one substation of the adopted LVDN, thereby for most nodes, $S(i)$ is empty. Equation (B.6) outlines the composition of active power load, including electric vehicles' uncontrolled charging (often termed "dumb charging") loads, smart charging loads, heating loads, and other electrical loads such as washing machines. The voltage drops between the starting and ending nodes of a power line due to line impedance is represented by Constraint (B.7). The maximum and minimum allowable voltages are imposed by Constraint (B.8). Constraints (B.9-B.10) provide capacity limits for lines and substations. Constraint (B.11) stipulates that the photovoltaic output must be non-negative and no greater than the available photovoltaic generation.

$$\sum_{l \in L_s(i)} P_{l,t} - \sum_{l \in L_e(i)} P_{l,t} = \sum_{s \in S(i)} P_{s,t}^{sub} + P_{i,t}^{PV} + P_{i,t}^{batt} + P_{i,t}^{V2G} - P_{i,t}^{load} \quad \forall t, \forall i \tag{B.4}$$

$$\sum_{l \in L_s(i)} Q_{l,t} - \sum_{l \in L_e(i)} Q_{l,t} = \sum_{s \in S(i)} Q_{s,t}^{sub} - Q_{i,t}^{load} \quad \forall t, \forall i \tag{B.5}$$

$$P_{i,t}^{load} = P_{i,t}^{EV,dumb} + P_{i,t}^{EV,smart} + P_{i,t}^{heat} + P_{i,t}^{other} \quad \forall t, \forall i \tag{B.6}$$

$$V_{s(l),t}^2 - V_{e(l),t}^2 = 2 r_l P_{l,t} + 2 x_l Q_{l,t} \quad \forall t, \forall l \tag{B.7}$$

$$\underline{V}_i \leq V_{i,t} \leq \overline{V}_i \quad \forall t, \forall i \tag{B.8}$$

$$S_{l,t} = \sqrt{P_{l,t}^2 + Q_{l,t}^2} \leq \overline{S}_l \quad \forall t, \forall l \tag{B.9}$$

$$S_{s,t}^{sub} = \sqrt{\left(P_{s,t}^{sub}\right)^2 + \left(Q_{s,t}^{sub}\right)^2} \leq \overline{S}_s^{sub} \quad \forall t, \forall s \tag{B.10}$$

$$0 \leq P_{i,t}^{PV} \leq \overline{P}_{i,t}^{PV} \quad \forall t, \forall i \tag{B.11}$$

Operational constraints for battery storage of the first-stage model. The operational constraints for battery storage are stated in Constraints (B.12-B.14). Equation (B.12) defines the electricity output of battery storage, which is determined by the difference between the corresponding discharging power and the charging power. Equation (B.13) establishes the relationship in stored energy change between adjacent hours. This constraint also ensures that the stored energy in each battery storage at the end of the operating period reverts to its initial value. Constraint (B.14) sets the upper and lower bounds for $P_{i,t}^{D,batt}$, $P_{i,t}^{C,batt}$, and $E_{i,t}^{batt}$.

$$P_{i,t}^{batt} = P_{i,t}^{D,batt} - P_{i,t}^{C,batt} \quad \forall t, \forall i \tag{B.12}$$

$$E_{i,t}^{batt} - E_{i,t-1}^{batt} = \eta^C P_{i,t}^{C,batt} - P_{i,t}^{D,batt} \Big/ \eta^D, \quad E_{i,T}^{batt} = E_{i,init}^{batt} \quad \forall t, \forall i \tag{B.13}$$

$$0 \le P_{i,t}^{D,batt} \le \overline{P}_i^{batt}, \quad 0 \le P_{i,t}^{C,batt} \le \overline{P}_i^{batt}, \quad 0 \le E_{i,t}^{batt} \le \overline{E}_i^{batt} \quad \forall t, \forall i \tag{B.14}$$

Operational constraints for flexible loads of first-stage model. The operational constraints for batteries in EVs offering vehicle-to-grid services are similar to those of the battery storage and are stated in Constraints (B.15-B.17). The main difference between EV batteries and stationary battery storage is that EVs connect to the power grid only during specific times. An EV has a specific time to connect to the grid, with an entry moment and an exit moment. Typically, EVs plug into the grid when they return home in the afternoon or evening and unplug when they leave in the morning. Equation (B.15) defines the electricity output of EV batteries, which is determined by the difference between the corresponding discharging and charging powers. Equation (B.16) describes the change in stored energy from one hour to the next for EV batteries. This constraint also sets the initial energy when connecting to the grid and the target energy when leaving the grid. Constraint (B.17) sets the upper and lower bounds for $P_{i,t}^{D,V2G}$, $P_{i,t}^{C,V2G}$, and $E_{i,t}^{V2G}$. The flexibility provided by shiftable loads (including heating loads and other loads like washing machines) is also taken into account, allowing for the shifting of electricity consumption from one time to another. For any given node and specific hour, $P_{i,t}^{heat}$ and $P_{i,t}^{other}$ are no longer fixed constants but can be adjusted within certain limits, as illustrated by Constraint (B.18). Constraint (B.19) signifies that over the entire operating period, since the load is only shifted from one time to another, the total amounts of heating loads and other loads remain unchanged before and after the shifting.

$$P_{i,t}^{V2G} = P_{i,t}^{D,V2G} - P_{i,t}^{C,V2G}, \quad \forall i, \forall t \in \left[1, t_i^{out}\right] \cup \left(t_i^{in}, T\right] \tag{B.15}$$

$$E_{i,t}^{V2G} = E_{i,t-1}^{V2G} + \eta^C P_{i,t}^{C,V2G} - P_{i,t}^{D,V2G} \Big/ \eta^D, \quad E_{i,t_i^{in}}^{V2G} = E_{i,init}^{V2G}, \quad E_{i,t_i^{out}}^{V2G} = E_{i,target}^{V2G}, \quad \forall i, \forall t \in \left[1, t_i^{out}\right] \cup \left(t_i^{in}, T\right] \tag{B.16}$$

$$0 \le P_{i,t}^{D,V2G} \le \overline{P}_i^{V2G}, \quad 0 \le P_{i,t}^{C,V2G} \le \overline{P}_i^{V2G}, \quad 0 \le E_{i,t}^{V2G} \le \overline{E}_i^{V2G}, \quad \forall i, \forall t \in \left[1, t_i^{out}\right] \cup \left(t_i^{in}, T\right] \tag{B.17}$$

$$\underline{P}_{i,t}^{heat} \le P_{i,t}^{heat} \le \overline{P}_{i,t}^{heat}, \quad \underline{P}_{i,t}^{other} \le P_{i,t}^{other} \le \overline{P}_{i,t}^{other}, \quad \forall t, \forall i \tag{B.18}$$

$$\sum_{t=1}^{T} P_{i,t}^{heat} = \sum_{t=1}^{T} P_{i,t}^{heat,init}, \quad \sum_{t=1}^{T} P_{i,t}^{other} = \sum_{t=1}^{T} P_{i,t}^{other,init} \tag{B.19}$$

Data availability

Data will be made available on request.

References

[1] Cui RY, Hultman N, Cui D, McJeon H, Yu S, Edwards MR, et al. A plant-by-plant strategy for high-ambition coal power phaseout in China. Nat Commun 2021;12:1468.

[2] Kemp JM, Millstein D, Kim JH, Wiser R. Interactions between hybrid power plant development and local transmission in congested regions. Adv. Appl. Energy 2023;10:100133.

[3] 2022 Progress report to parliament: the CCC's annual assessment of UK progress in reducing emissions. Climate Change Committee; 2022. https://www.theccc.org.uk/wp-content/uploads/2022/06/Progress-in-reducing-emissions-2022-Report-to-Parliament.pdf.

[4] Net zero by 2050: a roadmap for the global energy sector. IEA; 2021. h.t.tps://iea.blob.core.windows.net/assets/deebef5d-0c34-4539-9d0c-10b13d840027/NetZeroby2050-ARoadmapfortheGlobalEnergySector_CORR.pdf.

[5] Edwards MR, Garibay-Rodriguez J, Erickson JS, Shayan M, Tan JL, Shen X, Qiu Y, Liu P. Assessing inequities in electrification via heat pumps across the US. Joule 2024;8(12):3290–302.

[6] Bowermaster D, Alexander M, Duvall M. The need for charging: evaluating utility infrastructures for electric vehicles while providing customer support. IEEE Electrif. Mag. 2017;5:59–67.

[7] Bogdanov D, Farfan J, Sadovskaia K, Aghahosseini A, Child M, Gulagi A, et al. Radical transformation pathway towards sustainable electricity via evolutionary steps. Nat Commun 2019;10:1077.

[8] Ismael SM, Aleem SHA, Abdelaziz AY, Zobaa AF. State-of-the-art of hosting capacity in modern power systems with distributed generation. Renew Energy 2019;130:1002–20.

[9] McKenna R, Lilliestam J, Heinrichs HU, Weinand J, Schmidt J, Staffell I, Hahmann AN, Burgherr P, Burdack A, Bucha M, Chen R. System impacts of wind energy developments: key research challenges and opportunities. Joule 2025;9(1):101799.

[10] Kohlhepp P, Harb H, Wolisz H, Waczowicz S, Müller D, Hagenmeyer V. Large-scale grid integration of residential thermal energy storages as demand-side flexibility resource: a review of international field studies. Renew. Sustain. Energy Rev. 2019;101:527–47.

[11] Yang S, Gao HO, You F. Demand flexibility and cost-saving potentials via smart building energy management: opportunities in residential space heating across the US. Adv. Appl. Energy 2024;14:100171.

[12] Wan Y, Kober T, Schildhauer T, Schmidt TJ, McKenna R, Densing M. Conditions for profitable operation of p2x energy hubs to meet local demand with energy market access. Adv. Appl. Energy 2023;10:100127.

[13] Saif A, Khadem SK, Conlon MF, Norton B. Impact of distributed energy resources in smart homes and community-based electricity market. IEEE Trans Ind Appl 2022;59(1):59–69.

[14] Hamann HF, Gjorgiev B, Brunschwiler T, Martins LS, Puech A, Varbella A, Weiss J, Bernabe-Moreno J, Massé AB, Choi SL, Foster I. Foundation models for the electric power grid. Joule 2024;8(12):3245–58.

[15] Gorman W, Kemp JM, Rand J, Seel J, Wiser R, Manderlink N, Kahrl F, Porter K, Cotton W. Grid connection barriers to renewable energy deployment in the United States. Joule 2024;9(2):101791.

[16] Transmission entry capacity (TEC) register. nationalgridESO; 2023. https://data.nationalgrideso.com/connection-registers/transmission-entry-capacity-tec-register.

[17] Pascual J, Arcos-Aviles D, Ursúa A, Sanchis P, Marroyo L. Energy management for an electro-thermal renewable–based residential microgrid with energy balance forecasting and demand side management. Appl Energy 2021;295:117062.

[18] Jing R, Zhou Y, Wu J. Electrification with flexibility towards local energy decarbonization. Adv. Appl. Energy 2022;5:100088.

[19] Stavrakas V, Flamos A. A modular high-resolution demand-side management model to quantify benefits of demand-flexibility in the residential sector. Energy Convers. Manag. 2020;205:112339.

[20] Bedoya JC, Ostadijafari M, Liu CC, Dubey A. Decentralized transactive energy for flexible resources in distribution systems. IEEE Trans. Sustain. Energy 2020;12(2):1009–19.

[21] Li Y, Han M, Yang Z, Li G. Coordinating flexible demand response and renewable uncertainties for scheduling of community integrated energy systems with an electric vehicle charging station: a bi-level approach. IEEE Trans. Sustain. Energy 2021;12(4):2321–31.

[22] Jin X, Wu Q, Jia H. Local flexibility markets: literature review on concepts, models and clearing methods. Appl Energy 2020;261:114387.
[23] Arbabzadeh M, Sioshansi R, Johnson JX, Keoleian GA. The role of energy storage in deep decarbonization of electricity production. Nat Commun 2019;10:3413.
[24] Huang C, Wang C, Xie N, Wang Y. Robust coordination expansion planning for active distribution network in deregulated retail power market. IEEE Trans Smart Grid 2019;11(2):1476–88.
[25] Hayes BP, Thakur S, Breslin JG. Co-simulation of electricity distribution networks and peer to peer energy trading platforms. Int. J. Electr. Power Energy Syst. 2020; 115:105419.
[26] Zhou Y, Wu J, Long C. Evaluation of peer-to-peer energy sharing mechanisms based on a multiagent simulation framework. Appl Energy 2018;222:993–1022.
[27] Willems N, Rai V. Shareholder, regulatory, and social influence on firm behavior and energy market outcomes. Joule 2024;8(11):3017–37.
[28] Ruan G, Qiu D, Sivaranjani S, Awad AS, Strbac G. Data-driven energy management of virtual power plants: a review. Adv. Appl. Energy 2024;14:100170.
[29] van Ruijven BJ, De Cian E, Wing Sue. I. Amplification of future energy demand growth due to climate change. Nat Commun 2019;10:2762.
[30] Future energy scenarios. nationalgridESO; 2022. https://www.nationalgrideso.com/document/264421/download.
[31] Mu Y, Wu J, Jenkins N, Jia H, Wang C. A spatial–temporal model for grid impact analysis of plug-in electric vehicles. Appl Energy 2014;114:456–65.
[32] Mu Y, Wu J, Ekanayake J, Jenkins N, Jia H. Primary frequency response from electric vehicles in the Great Britain power system. IEEE Trans Smart Grid 2012;4 (2):1142–50.
[33] Thingvad A, Calearo L, Andersen PB, Marinelli M. Empirical capacity measurements of electric vehicles subject to battery degradation from V2G services. IEEE Trans. Veh. Technol. 2021;70(8):7547–57.
[34] Supplementary information for P2P-coordinated-flexibility paper Github; 2024. https://github.com/wgan6/P2P-coordinated-flexibility/blob/main/Supplementary%20information%20-%20ADAPEN.docx.
[35] Population of the united kingdom in 2021, by region. D. Clark; 2022. https://www.statista.com/statistics/294729/uk-population-by-region/.
[36] Long term development statement (LTDS) Table 3a observed peak demand. UK Power Networks; 2022. https://ukpowernetworks.opendatasoft.com/explore/dataset/ltds-table-3a-load-data-observed/table/?refine.licencearea=London+Power+Networks+(LPN).
[37] Network capacity map. National Grid; 2022. https://www.nationalgrid.co.uk/our-network/network-capacity-map-application.
[38] Demand heat map. Northern Powergrid; 2022. https://www.northernpowergrid.com/demand-availability-map.
[39] Network capacity. Scottish & Southern Electricity Networks; 2022. https://network-maps.ssen.co.uk/opendataportal.
[40] Our business plan for 2023-28. Northern Powergrid; 2021. https://ed2plan.northernpowergrid.com/sites/default/files/document-library/NPg_Our_business_plan_for_2023_28.pdf.
[41] United kingdom generic distribution system. Centre for Sustainable Electricity and Distributed Generation; 2015. https://github.com/sedg/ukgds.
[42] Urban demographics: where people live and work. Centre for Cities; 2015. https://www.centreforcities.org/wp-content/uploads/2015/07/15-07-20-Urban-Demographics.pdf.
[43] Household electricity survey: a study of domestic electrical product usage. Intertek Testing & Certification Ltd; 2012. https://assets.publishing.service.gov.uk/government/uploads/system/uploads/attachment_data/file/208097/10043_R66141HouseholdElectricitySurveyFinalReportissue4.pdf.
[44] Abeysinghe S, Wu J, Sooriyabandara M, Abeysekera M, Xu T, Wang C. Topological properties of medium voltage electricity distribution networks. Appl Energy 2018; 210:1101–12.
[45] Abeysinghe S, Abeysekera M, Wu J, Sooriyabandara M. Electrical properties of medium voltage electricity distribution networks. CSEE J. Power Energy Syst. 2020;7(3):497–509.
[46] Gan W, Zhou Y, Wu J. Quantifying grid flexibility provision of virtual vehicle-to-vehicle energy sharing using statistically similar networks. Appl Energy 2025;390: 125818.
[47] Ortega-Vazquez M. Optimal scheduling of electric vehicle charging and vehicle-to-grid services at household level including battery degradation and price uncertainty. IET Gener. Transm. Distrib. 2014;8(6):1007–16.